



City Research Online

City, University of London Institutional Repository

Citation: Demetriou, D., Nikitas, N. & Tsavdaridis, K. D. (2016). Performance of fixed-parameter control algorithms on high-rise structures equipped with semi-active tuned mass dampers. *The Structural Design of Tall and Special Buildings*, 25(7), pp. 340-354. doi: 10.1002/tal.1261

This is the published version of the paper.

This version of the publication may differ from the final published version.

Permanent repository link: <https://openaccess.city.ac.uk/id/eprint/27697/>

Link to published version: <https://doi.org/10.1002/tal.1261>

Copyright: City Research Online aims to make research outputs of City, University of London available to a wider audience. Copyright and Moral Rights remain with the author(s) and/or copyright holders. URLs from City Research Online may be freely distributed and linked to.

Reuse: Copies of full items can be used for personal research or study, educational, or not-for-profit purposes without prior permission or charge. Provided that the authors, title and full bibliographic details are credited, a hyperlink and/or URL is given for the original metadata page and the content is not changed in any way.

City Research Online:

<http://openaccess.city.ac.uk/>

publications@city.ac.uk

Performance of fixed-parameter control algorithms on high-rise structures equipped with semi-active tuned mass dampers

Demetris Demetriou, Nikolaos Nikitas* and Konstantinos Daniel Tsavdaridis

School of Civil Engineering, University of Leeds, Leeds, UK

SUMMARY

The present study investigates the performance of fixed parameter control algorithms on wind-excited high-rise structures equipped with semi-active tuned mass dampers of variable damping. It has been demonstrated that the algorithms that increase significantly the performance of the controlled structure do so at the expense of damper strokes. When the maximum damper strokes are capped to progressively lower limits, the efficacy of different algorithms, measured through a number of performance objectives, drastically alters totally changing the performance ranking of them and pointing out the need for an extensive study of the interplay between loading, control algorithm and allowable stroke within the design of semi-active tuned mass dampers devices. 2015 The Authors. *The Structural Design of Tall and Special Buildings* published by John Wiley & Sons Ltd.

Received 19 July 2015; Accepted 13 September 2015

KEY WORDS: vibration mitigation; control algorithms; wind engineering; high-rise buildings

1. INTRODUCTION

Since the introduction of the tuned mass damper (TMD) to the engineering community by Frahm in 1911 (Frahm, 1911), a large number of studies have been published validating the applicability and effectiveness of TMDs on high-rise and slender structures (Kawaguchi *et al.*, 1992; Xu *et al.*, 1992; Cao *et al.*, 1997; Sadek and Mohraz, 1998; Liu *et al.*, 2008; Casciati and Giuliani, 2009). In an attempt to improve further the effectiveness and flexibility of the device, researchers across the world have successfully altered the original design by incorporating sophisticated passive, semi-active and active elements. While the approach of upgrading the performance of the TMD using enhanced and innovative passive elements is reasonable from a technological, practical and economical perspective (Pinkaw and Fujino, 2001; Marian and Giaralis, 2014), this might not be always the case for semi-active and active control of structures because of the costs associated with the requirement of expensive actuators and specialized control components (such as electrorheological and magnetorheological dampers), which can be considered prohibitive for use on structural applications (Casciati *et al.*, 2012). Due to such limitations, over the years, an attempt has been made to improve the performance of actively and semi-actively controlled systems via the relatively easier design and selection of appropriate control algorithms, suitable for implementation in full-scale civil structures.

In the literature, most of the algorithms adopted for use on semi-active tuned mass dampers (STMD)-equipped structures are based on finding optimal control forces through the minimization of some cost function or performance index such as in the case of the linear quadratic regulator (LQR) and linear quadratic Gaussian (H2/LQG) control. Hrovat *et al.* (1983) were the first to suggest the use of variable damping dynamic absorbers on civil structures. They proposed an optimal control method for reducing the wind-induced vibration of a model two degrees of freedom (DOF) structure, demonstrating the superiority of the proposed system over a relevant traditional passive. Later, on a

*Correspondence to: Nikolaos Nikitas, School of Civil Engineering, University of Leeds, Leeds, UK.
E-mail: n.nikitas@leeds.ac.uk

similar study, Pinkaew and Fujino (2001) demonstrated the gains of the LQR-controlled STMD variable damping device on reducing the response of structures under harmonic excitations. They reported substantial improvements on the steady-state response of the structure around the tuning frequency, but only minor gains for the transient component of the vibration. Over the same years, ‘another class of optimal control laws’, the so-called bang-bang (BANG) control method has been investigated. Wu and Soong (1996) and Jansen and Dyke (2000) investigated the performance of optimal and suboptimal BANG controllers on semi-actively controlled structures, comparing their effectiveness against other algorithms on the benchmark of earthquake-excited structures. Later, Koo *et al.* (2004) developed a semi-active control algorithm, termed ‘groundhook control’ for use on STMD variable damping devices. This algorithm was developed as an extension to the ‘skyhook control’ algorithm proposed by Karnopp and Crosby (1974) for use on vehicle suspension systems. The flexibility of the former lies on its simplicity of implementation, its computational efficacy and its demand for only two sensors in order to achieve the calculation of control actions. Validating the effectiveness of the groundhook control scheme, Kang *et al.* (2011) examined the performance of different semi-active device configurations on wind excited tall structures, demonstrating that (displacement-based) groundhook-controlled STMD devices can substantially reduce the response of the structure when compared with passive TMD solutions. These authors also observed that using an optimally tuned displacement-based groundhook (DBG) controller, the predefined stroke limitations could not be satisfied; thus, an additional passive damper was required for satisfying the stroke limitations. Most recently, Demetriou *et al.* (2014) demonstrated that proportional-integral-derivative (PID) controllers can also be tailored for use on variable damping STMD-equipped structures subjected to earthquake excitations and outlined the benefits from the use of such a control strategy.

Even though all the quoted studies inarguably drew conclusions on the enhanced performance of the STMD-equipped system over its conventional passive analogue, it is evident that the once small and meaningless damper strokes (i.e. not being translated to practical applicable values) arising either due to the nature of the external perturbations (harmonic, white noise or short earthquake) and the system’s geometric and dynamic properties (low-rise and high-frequency structures) cannot be overlooked when it comes to high-rise structures subjected to long-term wind actions. For these reasons, no truly conclusive argument can be made regarding the relative performance of (a) STMD over TMD equipped structures and (b) the gains arising from different algorithms on high-rise structures equipped with STMD variable damping devices; particularly when the main performance-limiting factor is the stroke of the damper; this evidently needs to be taken into account for reaching any performance verdict.

Naturally in this study, the effectiveness of a variable damping STMD device on alleviating dynamic response of a benchmark high-rise structure is investigated, and the relative performance of five of the most popular fixed parameter feedback algorithms, namely the groundhook (DBG and velocity-based groundhook (VBG)), clipped optimal, BANG and PID controls, is reassessed. The dynamic input takes the form of a wind buffeting-type load, always of interest to high-rise buildings. Discussions on both quantitative and qualitative gains arising from the use of each control algorithm are sought, while at the same time, the fairness of all comparisons is explicitly preserved. As a novel feature, the possibility of switching to an appropriate algorithm for improving performance at the expense of low damper strokes is exploited in an attempt to avoid performance deterioration and cost due to the addition of an auxiliary damper when limited strokes are imposed.

2. MODELLING THE SEMI-ACTIVE TUNED MASS DAMPERS CONTROLLED SYSTEM

The dynamic behaviour of a generic, linear, controlled building structure modelled as a sway n -DOF lumped mass system when subjected to an arbitrary disturbance is fully captured by its matrix equation of motion as follows:

$$M\ddot{x}(t) + C\dot{x}(t) + Kx(t) = Bu(t) + Dd(t), \quad (1)$$

where M , C and K are the $n \times n$ mass, damping and stiffness matrices, respectively; $x(t)$ and $d(t)$ are in order the displacement and external force n -element vectors; $u(t)$ is a single scalar control force

calculated using an appropriate control algorithm; and B and D are the $n \times 1$ influence matrices assigning the control and external force contributions, respectively, to the individual DOFs. For each DOF in $x(t)$ being the displacement of the i^{th} ($i = 1, \dots, n$) mass, M trivially becomes diagonal, while for the specific viscous damping considered, the damping matrix C is assumed to have a form identical to the symmetric stiffness matrix K (i.e. classical damping approach). Without loss of generality, the system considered is equipped with a mass damper system attached to its $(n - 1)^{\text{th}}$ DOF, with the devices' motion variable constituting the n^{th} DOF. Adopting a state-space formulation, Eq. (1) becomes the following:

$$\dot{z}(t) = Az(t) + Fu(t) + Ed(t), \quad (2)$$

where $\dot{z}(t)$ represents the first-order time-change of the states $z(t) (= [x(t)\dot{x}(t)]^T)$ of the system; A is the system block matrix containing the system's mass, damping and stiffness properties; F is the control force locator block matrix; and E is the external perturbation locator block matrix, such that

$$A = \begin{bmatrix} 0 & I \\ -M^{-1}K & -M^{-1}C \end{bmatrix}, F = \begin{bmatrix} 0 \\ M^{-1}B \end{bmatrix}, E = \begin{bmatrix} 0 \\ M^{-1}D \end{bmatrix}, \quad (3)$$

with I being the identity matrix of appropriate dimensions (i.e. $n \times n$).

Unlike a conventional passive TMD equipped system that produces an unregulated control force as a result of the relative motion $(\dot{x}_r(t), x_r(t))$ of its mass against its supports (i.e. between the n^{th} and $(n - 1)^{\text{th}}$ DOFs) such that

$$u(t) = k_p x_r(t) + c_p \dot{x}_r(t), \quad (4)$$

where c_p and k_p are the passive damping and stiffness coefficients of the TMD; an STMD can be modulated damping-wise between two values, referred to as passive maximum (c_{\max}) and passive minimum (c_{\min}) as depicted in Figure 1. By employing a suitable control algorithm, the calculation of the appropriate maximum and minimum damping coefficients either directly or through the calculation

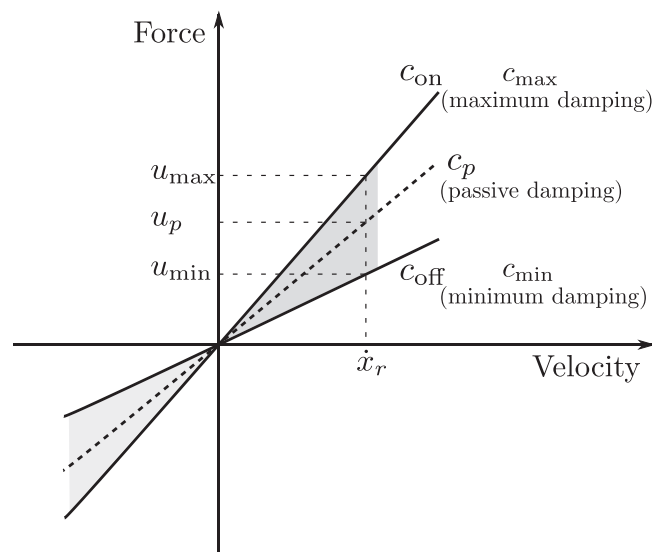


Figure 1. Force-velocity relationship for the performance bands of a variable damping device.

of a desired active force $u_a(t)$, one allows for enhanced overall energy dissipation capacity for the damper and improved performance of the vibration control system.

For the cases where a purely active algorithm such as the LQR or the PID is used for the calculation of c_{\max} and c_{\min} , the desired active force $u_a(t)$ needs to be calculated and tailored to an equivalent semi-active force, which can be physically realizable by the device. To this respect, because a semi-active device can, by definition, only consume energy, functioning criteria need to be applied on the active control force. Namely, the semi-active force $u_{sa}(t)$ is calculated by the following:

$$u_{sa}(t) = u_a(t) \left(\frac{1 - \text{sgn}[u_a(t)\dot{x}_r(t)]}{2} \right), \tag{5}$$

$$\text{sgn}[u_a(t)\dot{x}_r(t)] = \text{sgn}(q_a) = \begin{cases} 1 & \text{for } q_a \leq 0 \\ -1 & \text{for } q_a > 0 \end{cases}. \tag{6}$$

From this, the relevant power ‘dissipation’ of the semi-active device q_{sa} can be calculated by

$$q_{sa} = u_{sa}(t)\dot{x}_r(t) < 0, \tag{7}$$

where the negative sign is only indicating the flow of energy from the structure to the semi-active control device. Having obtained the physically attainable semi-active force, the time-varying semi-active damping coefficient $c_{sa}(t)$ can be directly calculated as follows:

$$c_{sa}(t) = \left| \frac{u_{sa}(t)}{\dot{x}_r(t)} \right|, \text{ where } c_{\min} \leq c_{sa}(t) \leq c_{\max}. \tag{8}$$

3. CONTROL ALGORITHMS

3.1. Groundhook control

Karnopp and Crosby (1974) in an attempt to reduce the response of vehicles using semi-active suspension systems developed the famous skyhook control scheme. In this approach, the directionality condition of the forces is examined in order to determine whether a high or a low state of damping is required. Obviously, contrary to civil engineering structural control, automotive engineering control systems primarily aim to control the sprung mass (i.e. the mass supported by the damper) instead of the unsprung mass (the mass supporting the mass damper), making skyhook control not suitable for use on STMD-equipped structures. To overcome this limitation, Koo *et al.* (2004) altered the original skyhook controller design and extended its application on civil structures equipped with STMD devices. The resulting scheme is known as groundhook control. In a groundhook control scheme, depending on the motion of the mass of the damper and the structure, and without the loss of generality, four cases are identified and damper forces are calculated in accordance to that in Table I.

Table I. Groundhook control logic

Sign conventions	Damper conditions	Desired damping state
$\dot{x}_{n-1} > 0, \dot{x}_r < 0$	Extension	Off
$\dot{x}_{n-1} > 0, \dot{x}_r > 0$	Compression	On
$\dot{x}_{n-1} < 0, \dot{x}_r < 0$	Extension	On
$\dot{x}_{n-1} < 0, \dot{x}_r > 0$	Compression	Off

Summarizing the conditions, the VBG control logic is mathematically captured by the following:

$$\text{if } \dot{x}_{n-1}\dot{x}_r \geq 0 \quad \therefore c_{sa}(t) = c_{\max}, \quad \text{if } \dot{x}_{n-1}\dot{x}_r < 0 \quad \therefore c_{sa}(t) = c_{\min}. \quad (9)$$

Alternatively, it is possible to replace the velocity of the unsprung mass by a primary system displacement term, resulting to DBG control, mathematically expressed as follows:

$$\text{if } x_{n-1}\dot{x}_r \geq 0 \quad \therefore c_{sa}(t) = c_{\max}, \quad \text{if } x_{n-1}\dot{x}_r < 0 \quad \therefore c_{sa}(t) = c_{\min}. \quad (10)$$

3.2. Proportional-integral-derivative control

A PID controller works on the basis of calculating appropriate control actions based on a calculated feedback error $e(t)$. For negative feedback control systems, the error $e(t)$ defined as the difference of the output signal $y(t)$ (i.e. displacement/velocity/accelerations) to a desired reference signal $r(t)$ is mathematically expressed as $e(t) = r(t) - y(t)$. It is noteworthy that for structural applications, the desired state is the equilibrium; thus, the reference signal $r(t)$ can take a value of zero. The controller's objective is to minimize the error for the next iteration by appropriately adjusting the inputs to the structure. Using the textbook version of the PID controller, the desired control inputs that minimize the feedback error are calculated by the following (Astrom and Murray, 2012):

$$u_a(t) = G_{pro}e(t) + G_{in}\int_0^{t_f} e(t)dt + G_d\frac{de(t)}{dx}. \quad (11)$$

The objective of the control algorithm is to calculate or tune the gains G_{pro} , G_{in} , G_d in such a way that given a feedback error at any time instant t within the control duration t_f , the generated inputs will result into enhanced vibration performance. Demetriou *et al.* (2014) have previously found that similarly to any active control algorithm tailored for use on semi-active systems, PID controllers can be tuned 'aggressively', i.e. allow for large gains that will minimize the rise-time and settling time for optimal semi-active control behaviour. The large gains will in turn generate large control forces that cannot be achieved by conventional active devices. Yet, due to the nature of semi-active control devices such as magneto-rheological (ME) and electro-rheological (ER) dampers with response times in the range of a few milliseconds and their ability to limit the desired force by only varying their damping coefficient, aggressive PID gain tuning can be considered as a viable optimal approach.

3.3. Bang-bang control

A BANG controller used within energy dissipation devices, in contrast to a groundhook controller, makes use of both the relative displacement and velocity of the two ends of the device for the derivation of the control action. When the relative velocity and displacement are in the same direction, the controller produces a force that increases the friction in the device, and in a manner work like a conventional brake that dissipates energy. When the relative velocity and displacement are in opposite directions, the force is eased in order to allow the device to move with reduced restriction. The control law can be mathematically expressed as:

$$\text{if } \text{sgn}(x_r) = -\text{sgn}(\dot{x}_r) \quad \therefore c_{sa}(t) = c_{\max}, \quad (12)$$

$$\text{if } \text{sgn}(x_r) = \text{sgn}(\dot{x}_r) \quad \therefore c_{sa}(t) = c_{\min}. \quad (13)$$

3.4. Linear quadratic regulator control

The LQR works on the basis of minimizing a quadratic performance index through manipulation and optimization of the control input. The performance index used in structural control applications when working with the state space formulation is defined as (Soong, 1990):

$$J = \int_0^{t_f} [z^T(t)Qz(t) + u(t)^T Ru(t)] dt. \quad (14)$$

In Eq. (14), Q and R are weighting matrices relating to the trade-off between control effectiveness and control energy consumption, respectively. By manipulating the magnitudes of Q and R , better vibration attenuation performance can be achieved at the expense of control effort (forces and energy demand) and vice versa. For example, a better disturbance rejection and minimization of the state error could be achieved by increasing the magnitude of the elements of the Q matrix relative to the R matrix. In contrast, increasing the magnitude of the R relative to the Q matrix would yield smaller control forces, thus less control effort as well as reduced disturbance rejection. The values of elements of these matrices are selected such that Q is a positive semi-definite matrix and R is a positive definite matrix. By doing so, Eq. (14) will never yield a negative result. Once the weighting matrices have been obtained, the problem reduces to the classical optimal problem where the control gain G is calculated by

$$G = -\frac{1}{2}R^{-1}F^T P, \quad (15)$$

where P is the Riccati matrix found by solving the algebraic Riccati equation:

$$PA - \frac{1}{2}PFR^{-1}F^T P + A^T P + 2Q = 0. \quad (16)$$

Using the calculated control gain, the control action is calculated by

$$u_a(t) = -Gz(t). \quad (17)$$

4. NUMERICAL INVESTIGATION

4.1. Structural configuration

To illustrate the effectiveness of the different algorithms at alleviating structural response, the 76-storey benchmark wind-sensitive structure proposed by Yang *et al.* (2004) is considered. The building has a square $42\text{ m} \times 42\text{ m}$ cross-section, with a height-to-width aspect ratio of 7.3 and a low natural frequency that lends it the wind-sensitivity attribute.

A simplified planar finite element model of the structure is constructed by considering the portion of the building between two adjacent rigid floors as a classical beam element of uniform thickness, leading to 76 rotational and 76 translational DOFs. From these, all the rotational DOFs have been removed using static condensation, leading to a lumped mass sway model with DOFs, representing the displacement of each floor in the lateral direction. The resulting simulated structure has a total mass of 153 000 t, with the first five frequencies at 0.16 Hz, 0.765 Hz, 1.992 Hz, 3.790 Hz and 6.395 Hz, and corresponding modal structural damping ratios of 1% calculated using Rayleigh's approach. The response of the structure under a predefined wind load was investigated for two structural configurations: (a) structural model with an optimally designed TMD and (b) with an STMD at different control algorithm configurations. A schematic representation of the two different structural configurations is presented in Figure 2.

Both the TMD and STMD devices comprise an inertial mass of 500 t that corresponds to 0.356% of the total structural mass. Because of the long period of the structural system and the associated motion generally governed by the first modal response, it was deemed appropriate to tune both the devices on the fundamental frequency of the structure (i.e. $\approx 1\text{ rad/s}$).

4.1.1. Wind excitation input

The wind excitation input is derived from wind tunnel tests performed on a rigid model of the 76-storey benchmark structure constructed and tested in the Department of Civil Engineering, at the University of Sydney, Australia. The wind velocities used in the tests were derived from

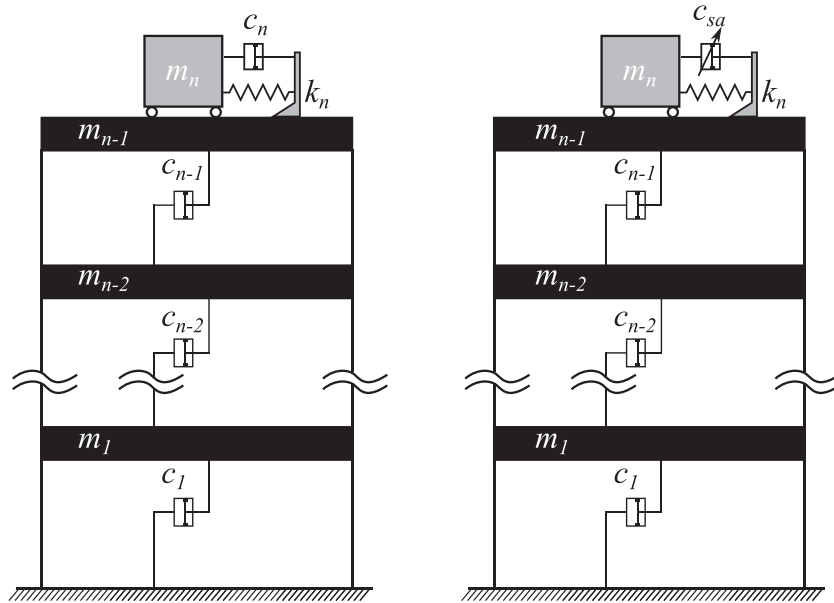


Figure 2. Ensemble of the structural configurations. (left) TMD-equipped structure and (right) STMD-equipped structure.

ASS1170.2-1989 (Australian Wind Code (Australian, 1989)) for winds with return period of 10 years. Thirty-two pressure panels (16 panels on either side of the test structure) were combined to give a single-pressure coefficient at the centre of each panel. The combined pressure coefficients are converted into across wind forces using:

$$F(t) = 0.5\rho U^2 C_{Pr}(t) A_{pan}, \quad (18)$$

where ρ is the density of air (kgm/m^3), U is the mean wind speed at the top of the building (m/s), A_{pan} is the corresponding single panel area (m^2) and $C_{Pr}(t)$ is the dimensionless instantaneous combined pressure coefficient (for more information on the exact details used for the derivation of the wind forces, the reader is referred to Samali *et al.*, 2004). Indicatively, Figure 3(a) and (b) illustrates the resulting dynamic part of the wind force for the first and last occupied floors along with the frequency content of each loading case. Evidently, any motion-correlated component is excluded from this wind force description (i.e. no interaction of the motion with the wind force is enabled).

4.2. Tuned mass damper and semi-active tuned mass damper damping tuning

To this date, most of the tuning of the mechanical parameters of a TMD device is achieved via closed-form expressions derived from the minimization of the rms acceleration response of a single degree of freedom (SDOF) subjected to white noise or harmonic excitation. While this approach is broadly accepted, representing civil engineering structures with an equivalent SDOF system can lead to significant errors in the estimation of their dynamic response. The problem amplifies when one considers the probabilistic nature of the knowledge of the system's properties and the fact that the estimated properties can vary with time (e.g. amplitude dependence, fluid-structure interaction etc.). Moreover, obtaining TMD mechanical parameters through the use of harmonic or flat spectrum inputs may not always yield optimum values (Ricciardelli *et al.*, 2000). For these reasons, in this paper, because the motion of long period structures is generally governed by the first modal response, both the TMD and STMD are tuned to the fundamental frequency of the structure. On the other hand, tentative damping values are given to the damping devices based on existing formulas found in literature

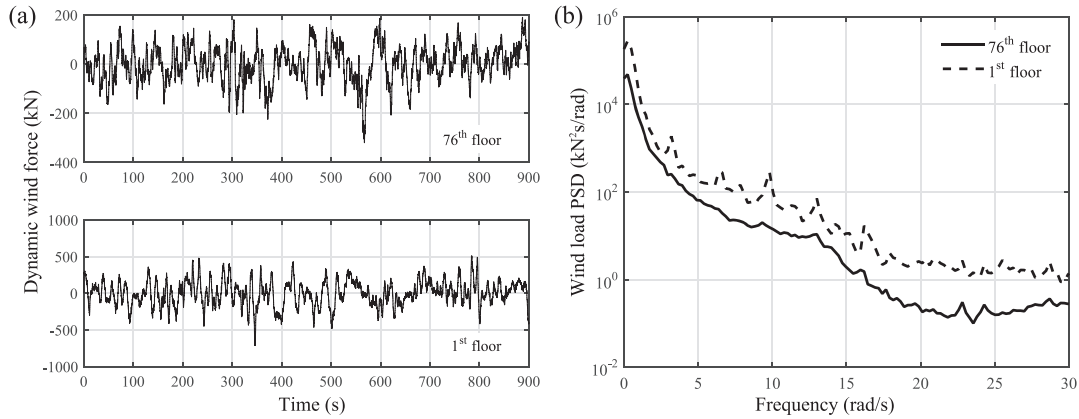


Figure 3. (a) Dynamic wind force time histories of last and first occupied floor and (b) frequency content of the wind excitation fluctuation.

(Hartog, 1956; Ghosh and Basu, 2007), validated and adjusted when necessary through numerical/response optimization on the multi degree of freedom (MDOF) system. Following this principle, the numerical optimization procedure is based on minimizing the root mean square (rms) structural acceleration response. Figure 4(a) shows the frequency response of the TMD-equipped structure under monoharmonic excitation around the tuning frequency of 1 rad/s for different damping ratios of the device, while Figure 4(b) shows the rms acceleration response of the structure at different floors, under wind excitation at the range of different damping ratios considered within Figure 4(a).

From these two figures, it is evident that under both harmonic and wind excitation, the TMD-equipped structure has a better performance when the damping ratio is between 3% and 5%. By employing a simplex search algorithm for iterative/numerical response optimization of the rms acceleration response of the wind-excited 76-storey structure, a damping ratio of 4.7% was selected for the later analysis.

Similar to obtaining the appropriate fixed damping ratio for the TMD device, numerical optimization using the Nelder–Mead simplex search algorithm (Nelder and Mead, 1965) was employed for deriving the maximum and minimum damping ratios for the STMD device. The implementation of the simplex algorithm was performed using MATLAB (MathWorks) response optimization toolbox. It is worth noting that similarly to the optimization of the TMD, the optimization of the STMD device is carried out solely on the basis of reducing the rms structural acceleration response of the last occupied floor (75th). Figure 5(a) and (b) shows how the algorithm alters non-uniformly the c_{max} and c_{min} values at each of its iterations in an attempt to minimize the rms acceleration metric.

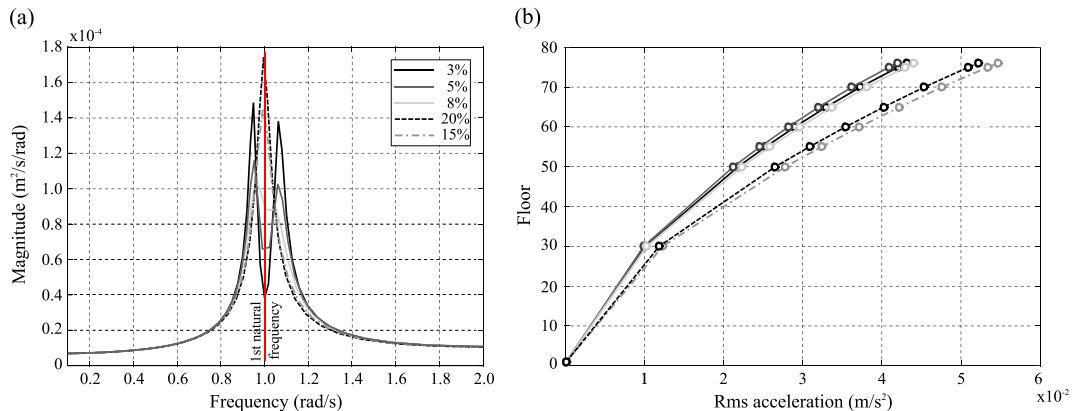


Figure 4. (a) Power spectral density of the acceleration of the 7th floor under harmonic loading and (b) rms acceleration response of different floors under the across wind loading derived from the static wind-tunnel tests.

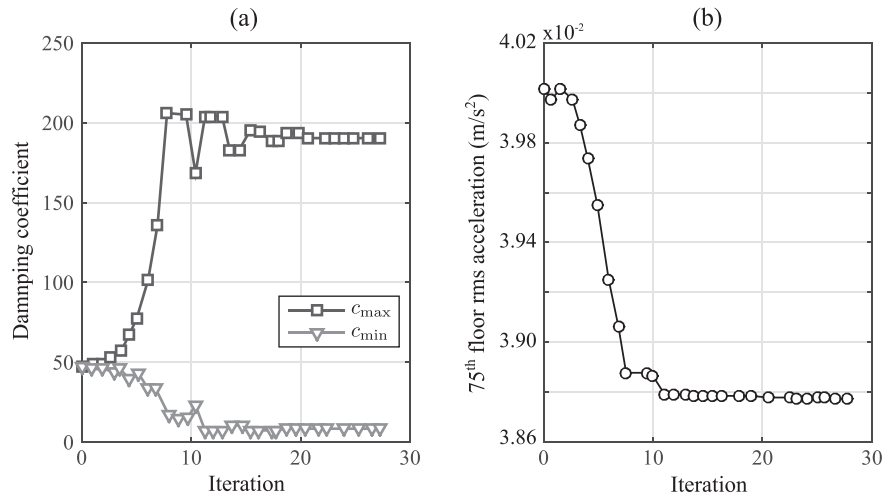


Figure 5. Numerical response optimization using the Nelder–Mead simplex method. (a) damping band convergence and (b) rms response convergence.

Figure 6 shows the resulting damping ratios for each algorithm configuration on the STMD-equipped system, along with the damper strokes obtained from the response optimization procedure. It is important to notice that the device stroke was implemented as an additional variable to the problem in order to study the stroke limitations and interactions with the overall vibration mitigation performance it enables. The same scale was used throughout for comparative assessments.

It can be observed that as the stroke of the damper is progressively reduced, some of the algorithms could not achieve enhanced performance compared with the TMD-equipped system with respect to the optimization variable (rms acceleration). The phrase ‘not-attainable’ in Figure 6 is used to graphically illustrate the aforementioned argument. In this respect, ‘not-attainable’ demonstrates that the optimization of the LQR-STMD ensemble for strokes ≤ 80 cm, both minimum and maximum damping ratios converge to that of the TMD. Similarly, the DBG, LQR and PID control STMD ensembles for damper strokes ≤ 75 cm converge to the same minimum and maximum damping ratios of the passive TMD.

In addition to the aforementioned observations, the results of the optimization suggest that two categories of algorithms can be distinguished. Namely these are a category of algorithms requiring a large high/low damping ratio (i.e. c_{max}/c_{min}) with a high c_{max} coefficient and a category of algorithms that requires a small high/low damping ratio with relatively low c_{max} coefficient. In the former category, the DBG, PID and LQR algorithms are found, while the latter category contains the remaining two algorithms, the VBG and BANG.

4.3. Evaluation criteria

The comparison of the different control algorithms is based on the stationary response properties of the different controlled structures. Although the response of the system is primarily governed by the first mode of vibration, the rms and peak accelerations and displacements at different storeys extracted from the associated time-histories are used in order to capture the participation of different modes to the structural response. From the obtained values, 12 performance criteria were identified. The first criterion, J_1 , appraises the ability of the control strategy to reduce rms accelerations at different building heights:

$$J_1 = \max(\sigma_{\ddot{x}_1}, \sigma_{\ddot{x}_{30}}, \sigma_{\ddot{x}_{50}}, \sigma_{\ddot{x}_{55}}, \sigma_{\ddot{x}_{60}}, \sigma_{\ddot{x}_{65}}, \sigma_{\ddot{x}_{70}}, \sigma_{\ddot{x}_{75}}) / \sigma_{\ddot{x}_{75o}}, \quad (19)$$

where $\sigma_{\ddot{x}_i}$ is the rms acceleration of the i^{th} storey and $\sigma_{\ddot{x}_{75o}}$ is the rms acceleration of the 75th floor (last occupied floor) without any control action. The second performance criterion evaluates the average performance of six floors above the 49th floor:

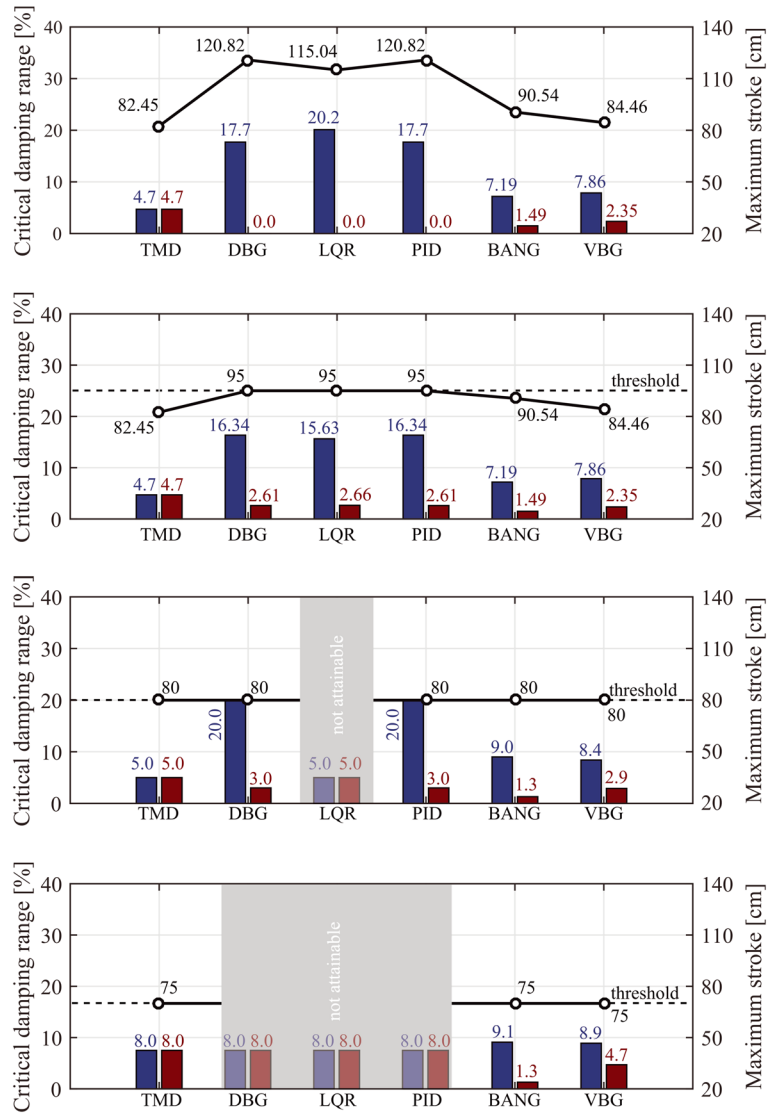


Figure 6. Optimal damping maximum–minimum ranges and damper strokes for the different STMD control scenarios for the cases (top to bottom) of uncapped damper strokes, strokes capped at 95 cm, 80 cm and 75 cm.

$$J_2 = \frac{1}{6} \sum_i (\sigma_{xi} / \sigma_{xio}), \text{ for } i = 50, 55, 60, 65, 70, 75, \tag{20}$$

where σ_{xio} is the rms of the i^{th} floor without control. The third and fourth performance indices assess the ability of the control system to reduce top floor displacements:

$$J_3 = \sigma_{x76} / \sigma_{x76o}, \tag{21}$$

$$J_4 = \frac{1}{7} \sum_i (\sigma_{xi} / \sigma_{xio}), \text{ for } i = 50, 55, 60, 65, 70, 75, \tag{22}$$

where σ_{xi} is the rms displacement of the i^{th} floor, σ_{xio} is the rms displacement of the i^{th} storey without control and σ_{x76o} is the rms displacement of the 76th floor without control. The fifth and sixth indices take into account the rms stroke of the damper and the average power, respectively:

$$J_5 = \sigma_{xm} / \sigma_{x76o}, \quad (23)$$

$$J_6 = \left\{ \frac{1}{t_f} \int_0^{t_f} [\dot{x}_m(t)u(t)]^2 dt \right\}^{1/2}, \quad (24)$$

in which σ_{xm} is the rms stroke of the damper, $\dot{x}_m(t)$ is the damper velocity and t_f is the total time of integration. Similarly to the first performance indices, the next four criteria (i.e. J_7 to J_{10}) evaluate the performance in terms of peak response quantities as follows:

$$J_7 = \max(\ddot{x}_{p1}, \ddot{x}_{p30}, \ddot{x}_{p50}, \ddot{x}_{p55}, \ddot{x}_{p60}, \ddot{x}_{p65}, \ddot{x}_{p70}, \ddot{x}_{p75}) / \ddot{x}_{p75o}, \quad (25)$$

$$J_8 = \frac{1}{6} \sum_i (\ddot{x}_{pi} / \ddot{x}_{pio}), \text{ for } i = 50, 55, 60, 65, 70, 75, \quad (26)$$

$$J_9 = x_{p76} / x_{p76o}, \quad (27)$$

$$J_{10} = \frac{1}{7} \sum_i (x_{pi} / x_{pio}), \text{ for } i = 50, 55, 60, 65, 70, 75, 76, \quad (28)$$

where \ddot{x}_{pi} is the peak absolute acceleration of the i^{th} floor with control and \ddot{x}_{pio} is the peak acceleration of the i^{th} floor without control. Similarly, x_{pi} is the peak displacement of the i^{th} floor and x_{pio} is the peak displacement of the i^{th} floor without control. The 11th criterion assesses the ability of the control strategy to minimize the stroke of the damper as follows:

$$J_{11} = x_{pm} / x_{p76o}, \quad (29)$$

in which x_{pm} is the peak stroke of the actuator. The last criterion examines the control effort by calculating the maximum required power by

$$J_{12} = \max|\dot{x}_m(t)u(t)|. \quad (30)$$

From the above defined criteria, it can be observed that the better the performance, the smaller the performance indices J_1, J_2, \dots, J_{12} (Yang *et al.*, 2004). Table II summarizes the 12 performance criteria introduced for the benchmark problem at hand.

5. SIMULATION RESULTS

Two structural configurations consisting of passive and semi-active control devices are used for investigating the performance of five different control algorithms on semi-actively controlled high-rise structures. Numerical optimization of the damping ratios for the TMD and STMD is carried out at different damper stroke states as described in Section 4.2. The optimized devices are incorporated to the benchmark problem for numerical simulation. From this, the obtained structural response properties are used to calculate the 12 predefined performance indices for four different damper stroke cases. Figures 7–10 present the results of the comparison. In these figures, the performance indices J_1 to J_4 and J_7 to J_{10} are associated with rms and peak response properties, respectively, while the remaining four performance indices J_5 , J_6 , J_{11} and J_{12} are associated with the stroke and the power consumed by the device.

Table II. Summary of performance criteria.

Index	Description
J_1	Maximum floor rms acceleration (among a floor selection)
J_2	Average rms acceleration for selected floors
J_3	Maximum rms displacement of top floor
J_4	Average rms displacement for selected floors
J_5	Rms actuator stroke
J_6	Rms control power
J_7	Maximum floor peak acceleration (among a floor selection)
J_8	Average peak acceleration for selected floors
J_9	Maximum peak displacement of top floor
J_{10}	Average peak displacement for selected floors
J_{11}	Peak actuator stroke
J_{12}	Peak control power

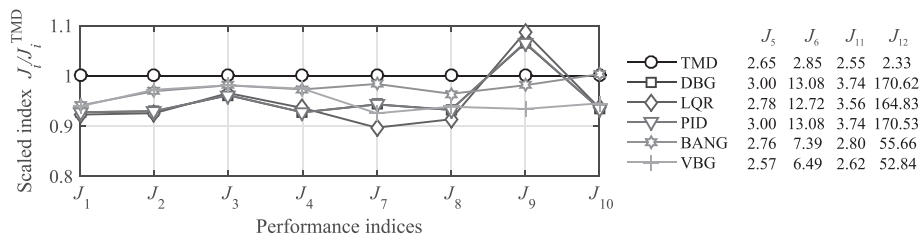


Figure 7. Scaled (over the TMD performance) performance indices $J_1, \dots, J_4, J_7, \dots, J_{10}$ for uncapped damper strokes.

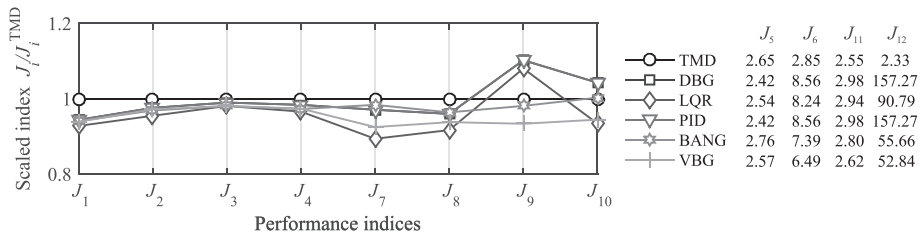


Figure 8. Scaled (over the TMD performance) performance indices $J_1, \dots, J_4, J_7, \dots, J_{10}$ for damper strokes ≤ 95 cm.

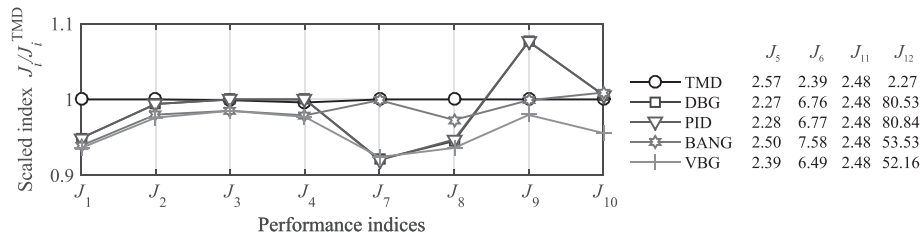


Figure 9. Scaled (over the TMD performance) performance indices $J_1, \dots, J_4, J_7, \dots, J_{10}$ for damper strokes ≤ 80 cm.

As probably expected, when the stroke of the damper is unrestrained the performance of the STMD-equipped structure at any control algorithm, configuration is superior on the majority of the performance objectives to that of the TMD-equipped one. This is illustrated through the lower values attained by performance indices J_1 to J_4 and J_7 to J_{10} excluding J_9 . Note that for illustrative purposes, a scaled form was opted for all later graphs whereby the performance is scaled over the TMD performance.

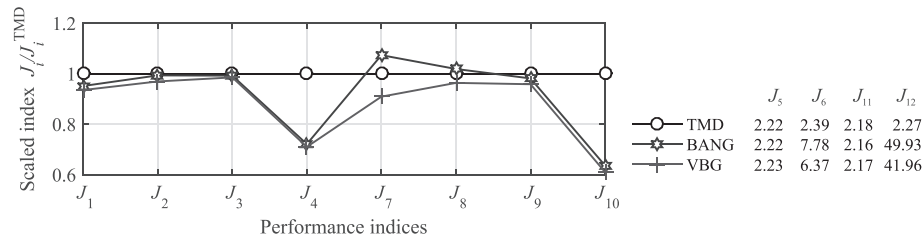


Figure 10. Scaled (over the TMD performance) performance indices $J_1, \dots, J_4, J_7, \dots, J_{10}$ for damper strokes ≤ 70 cm.

For the comparison between the different semi-active control configurations, the results from the uncapped damper stroke case indicate that it would be appropriate to divide the control algorithms into two categories. The first category contains the more ‘aggressive’ algorithms, indicated by a higher performance index J_{11} , and the second category of less ‘aggressive’ or more conservative algorithms that achieve performance gains at the expense of lower damper strokes (see also Figure 6 in its uncapped variant). In this regard, the DBG, LQR and PID controllers are termed ‘least-conservative’, while the BANG and VBG controllers are termed ‘conservative’. Subsequently, when considering rms response properties (indicated by J_1 to J_4), there is a noticeable difference between conservative and least conservative algorithms. As a matter of fact, the latter category of algorithms achieves rms response reduction ranging from 6% to 8% when compared with the TMD-equipped structure and from 3% to 5% when compared with the STMD-equipped structure coupled with conservative algorithms. On the other hand, when peak response properties are considered (indicated by J_7 to J_{10}), conservative algorithms better match the performance of least conservative ones and even show superior performance when peak top floor displacements are considered (indicated by J_9). It can be also observed that ‘aggressive’ tuning of the PID controller (as explained in Section 3.2), makes the system behave identically to the system ensemble with a DBG controller. Nevertheless, different PID tuning methods for optimal behaviour are not exploited in this paper; thus, conclusions on the similarity of PID to other control algorithms cannot be definitive.

By restraining the damper stroke to a maximum allowable value of 95 cm as suggested by Yang *et al.* (2004), with reference to Figure 8, it can be observed that conservative algorithms succeed in reaching the performance of least conservative algorithms and even noticeably surpassing it in the case of peak response values, with the only exception of the LQR that appears to be more robust to the drop of damper strokes, maintaining better rms and peak response performance than every other algorithm. By further reducing the stroke to ≤ 80 cm (Figure 9), similar observations can be made. However, the LQR that initially showed to be robust to the reduction of damper strokes failed to produce control actions that reduce the rms response of the structure without exceeding the stroke limit. This is evident from the fact that during the optimization, both damping coefficients c_{\max} and c_{\min} of the STMD device converged to a value of 4.7%, which is the optimum damping coefficient for the TMD device. In other words, at these (low) damper strokes, the LQR ensemble STMD cannot exceed the performance of a passive TMD with respect to the tuning property (rms acceleration). From the two conservative algorithms, the VBG shows better performance when compared with BANG both in terms of rms and peak responses

For damper strokes ≤ 70 cm, none of the least conservative algorithms is able to produce control actions that will reduce the performance objective set in Section 4.2. From the two remaining conservative algorithms, VBG remains preminent, while the BANG-STMD ensemble demonstrated inferior performance compared with the TMD system with respect to peak acceleration response properties indicated by performance index J_7 and J_8 .

From the above findings and with reference back to Figure 6, it is evident that regardless of the damper stroke, all three of the least conservative algorithms require high c_{\max} damping ratios for achieving optimum performance, while their c_{\min} coefficient is set to a relatively low value. This observation suggests that least conservative algorithms make better use of the minimum damping ratio for increasing stroke (and thus optimally increase the velocity of the damper so that the damping force is also increased), and thoroughly use their high damping only when necessary. This is similar to reducing the damping ratio of the passive device (thus increasing the stroke) up to a point where no more performance can be gained. Supporting this observation, the results obtained from the optimization of

minimum and maximum damping ratios for the cases of damper strokes ≤ 95 cm, least conservative algorithms restrain the stroke by increasing the c_{\min} coefficient while at the same time attempt to maintain the c_{\max} coefficient close to the optimal. Undoubtedly, in order to maintain the performance of least conservative algorithms close to the optimal, the resulting large c_{\max} dictates the requirement of large forces (and in turn control power indicated by performance index J_6 and J_{12}), which in turn influence the size and number of devices required for control.

6. CONCLUDING REMARKS

A variety of fixed parameter control algorithms proposed for semi-actively controlled structural systems have been evaluated for use on high-rise structures incorporating STMD devices, through numerical simulations on a wind-excited 76-storey benchmark structure. The implementation of each algorithm was conducted based on available measurements of the structural system including absolute accelerations, displacements and velocities. The STMD-equipped structure at each of the algorithm configurations resulted in an improved performance when compared with the best passive case, with only exception the case of peak displacements in which the passive system was superior to the semi-active one. Still, for the semi-active case, the response of the structure varied significantly, depending on the choice of algorithm. In this regard, it is found that when no consideration is given on the damper strokes, three of these algorithms are found to be most suited for use with STMD on wind-excited structures. The LQR, the DBG and the PID that maximize damper strokes, thus termed 'least-conservative', achieved significant response reductions. On the other hand, it has been demonstrated that by progressively reducing the damper strokes, the remaining two algorithms, the VBG and BANG, the algorithms that significantly restrain the damper strokes and thus termed 'conservative' managed to reach and even surpass in some cases the performance of previously 'best' algorithms. From the category of least conservative algorithms, the LQR was shown to be more effective for use on the structure of interest, yet the requirement for full state feedback that translates to additional state measurements and computational burdens suggests that DBG and PID might be practically superior. From the category of conservative algorithms, the VBG is shown to be unconditionally superior to the BANG. From this, it has been demonstrated that appropriate selection of a control algorithm can be considered as an alternative method of limiting damper strokes while maintaining expedient performance without the requirement of an external auxiliary damping device for limiting the stroke.

Finally, by investigating the tuning of the damping ratios for the different configurations, it is found that the main difference of the two categories of control algorithms is the requirement of the least conservative algorithms for high damping ratios for achieving optimal behaviour, whereas conservative algorithms require significantly lower values. As a matter of fact, for relatively similar performance gains, a DBG would require a maximum damping ratio of 16% as opposed to 8% required by a VBG. This suggests that the choice of an algorithm from the latter category would translate to a reduced size/number of auxiliary devices used, control forces and power, which in turn relate back to the practical applicability and cost of the STMD device on high-rise structures.

ACKNOWLEDGEMENTS

The authors gratefully acknowledge EPSRC, UK (Grant No.EP/L504993/1) and the University of Leeds for the financial support to this study.

REFERENCES

- Astrom KJ, Murray RM. 2012. *Feedback Systems—An Introduction for Scientists and Engineers*. Princeton University Press: New Jersey.
- Australian S. 1989. Minimum Design Loads on Structures. II: Wind Loads. *AS1170.2-1989*.
- Cao H, Reinhorn AM, Soong TT. 1997. Design of an active mass damper for a tall tv tower in Nanjing China. *Engineering Structures* **20**: 134–143.
- Casciati F, Giuliani F. 2009. Performance of multi-TMD in the towers of suspension bridges. *Journal of Vibration and Control* **15**: 821–847.

- Casciati F, Rodellar J, Yildirim U. 2012. Active and semi-active control of structures—theory and applications: a review of recent advances. *Journal of Intelligent Material Systems and Structures* **23**: 1181–1195.
- Demetriou D, Nikitas N, Tsavdaridis KD. 2014. Performance of proportional-integral-derivative controlled variable damping tuned mass dampers. Proceedings of the 6th International Conference of Structural Control, July, Barcelona, Spain.
- Frahm H. 1911. *Device for damping vibration of bodies*. United States patent application. Patent number 989 958.
- Ghosh A, Basu B. 2007. A closed-form optimal tuning criterion for TMD in damped structures. *Structural Control and Health Monitoring* **14**: 681–692.
- Hartog D. 1956. *Mechanical Vibrations*. McGraw-Hill Book Company: New York.
- Hrovat D, Barak P, Rabins M. 1983. Semi-active versus passive or active tuned mass dampers for structural control. *Journal of Engineering Mechanics, ASCE* **109**: 691–705.
- Jansen M, Dyke SJ. 2000. Semi-active control strategies for MR dampers: a comparative study. *Journal of Engineering Mechanics, ASCE* **126**: 795–803.
- Kang J, Kim HS, Lee DG. 2011. Mitigation of wind response of a tall building using semi-active tuned mass dampers. *The Structural Design of Tall and Special Buildings* **20**: 552–565.
- Karnopp DC, Crosby MJ. 1974. Vibration control using semi-active force generators. *Journal of Engineering for Industry* **5**: 619–626.
- Kawaguchi A, Teramura A, Omote Y. 1992. Time history response of a tall building with tuned mass damper under wind force. *Journal of Engineering and Industrial Aerodynamics*. **41-44**: 1949–1960.
- Koo JH, Murray TM, Setareh M. 2004. In search of suitable control methods for semi-active tuned vibration absorbers. *Journal of Vibration and Control* **10**: 163–174.
- Liu MY, Chiang WL, Hwang JH, Chu CR. 2008. Wind induced vibration of high-rise building with tuned mass damper including soil structure interaction. *Journal of Wind Engineering and Industrial Aerodynamics* **96**: 1092–1102.
- Marian L, Giaralis A. 2014. Optimal design of a novel tuned mass–damper–inertor (TMDI) passive vibration control configuration for stochastically support-excited structural systems. *Probabilistic Engineering Mechanics* **38**: 158–164.
- Nelder J, Mead R. 1965. A simplex method for function minimization. *Computer Journal* **7**: 308–313.
- Pinkaew T, Fujino Y. 2001. Effectiveness of semi-active tuned mass dampers under harmonic excitation. *Engineering Structures* **23**: 850–856.
- Ricciardelli F, Occhiuzzi A, Clemente P. 2000. Semi-active tuned mass damper control strategy for wind-excited structures. *Journal of Wind Engineering and Industrial Aerodynamics* **88**: 57–74.
- Sadek F, Mohraz B. 1998. Semiactive control algorithms for structures with variable dampers. *Journal of Engineering Mechanics* **981-990**.
- Samali B, Kwok K, Wood G, Yang J. 2004. Wind tunnel tests for wind-excited benchmark building. *Journal of Engineering Mechanics, ASCE* **130**: 447–450.
- Soong TT. 1990. *Active Structural Control: Theory and Practice*. John Wiley & Sons: New York.
- Wu Z, Soong TT. 1996. Modified bang-bang control law for structural control Implementation. *Journal of Engineering Mechanics, ASCE* **122**: 771–777.
- Xu YL, Samali B, Kwok KC. 1992. Control of along-wind response of structures by mass and liquid dampers. *Journal of Engineering Mechanics* **118**: 20–39.
- Yang NY, Agrawal AK, Samali B, Wu JC. 2004. Benchmark problem for response control of wind-excited tall buildings. *Journal of Engineering Mechanics, ASCE* **130**: 437–446.

AUTHORS' BIOGRAPHIES

Demetris Demetriou is a senior PhD student in structural dynamics and control at the School of Civil Engineering at the University of Leeds, UK. He received his MEng and BEng in structural engineering from the University of Leeds in 2013. His research interests include structural control, health monitoring and identification analysis.

Nikolaos Nikitas is a lecturer on structural dynamics at the School of Civil Engineering of the University of Leeds, UK. He received two PhDs, one from the University of Edinburgh and one from the University of Bristol. His expertise lies within the fields of aeroelasticity, structural health monitoring, inverse analysis and dynamic modelling of structures, while he is also fond of studies relevant to complexity and chaos.

Konstantinos Daniel Tsavdaridis is a lecturer on structural engineering in the School of Civil Engineering at the University of Leeds, UK. He holds an MSc and DIC in structural engineering from the Imperial College, London, and a PhD from the City University London. He specializes on design optimization of steel and composite structural systems and members developing sustainable innovative solutions, and on seismic-resistant design of lightweight steel and steel-concrete composite structures.